A MATHEMATICAL MODEL TO PREDICT THE EVOLUTION OF RETINAL NERVE FIBER LAYER THINNING IN MULTIPLE SCLEROSIS PATIENTS

Alberto Montolío[1,2], José Cegoñino[1,2], Elvira Orduna[3,4], Berta Sebastian[5], Elena Garcia-Martin[3,4], Amaya Pérez del Palomar[1,2*]

[1]Group of Biomaterials, Aragon Institute of Engineering Research (I3A), University of Zaragoza, Zaragoza, Spain

[2]Department of Mechanical Engineering, University of Zaragoza, Zaragoza, Spain

[3]Ophthalmology Department, Miguel Servet University Hospital, Zaragoza, Spain

[4]GIMSO Research and Innovative Group, Aragon Institute for Health Research (IIS Aragón), Zaragoza, Spain.

[5]Neurology Department, Miguel Servet University Hospital, Zaragoza, Spain

*Corresponding author:

Amaya Pérez del Palomar

C/Maria de Luna s/n, 50018 Zaragoza, Spain

Email: amaya@unizar.es

ABSTRACT

Multiple sclerosis (MS) is a neurodegenerative disease of the central nervous system (CNS). Many studies of MS patients have described axonal loss in the optic nerve of the retina, and specifically progressive thinning of the retinal nerve fiber layer (RNFL). We hypothesize that RNFL thinning involves the participation of 2 processes that cause CNS damage: autoimmune inflammation and axonal degeneration. To test this hypothesis, we developed a mathematical model based on ordinary differential equations to relate the evolution of RNFL thickness (measured by optical coherence tomography [OCT]) with that of the Expanded Disability Status Scale (EDSS) score in MS patients. Data were obtained from a longitudinal study of 114 MS patients who were followed-up for 10 years. After adjusting the parameters using a genetic algorithm, the model's prediction of the evolution of RNFL thickness accurately reflected the progression revealed by the 10-year clinical data. Our findings suggest that differences in the relative contributions of autoimmune inflammation and axonal degeneration can account for the complex dynamics of MS, which vary from one patient to the next. Moreover, our results show that CNS damage occurs cumulatively from the onset of MS and that most RNFL thinning occurs before the appearance of significant disability. RNFL thickness could therefore serve as a reliable biomarker of MS disease course. Our proposed methodology would enable the use of OCT data from new MS patients to predict the evolution of RNFL thinning and hence the progression of MS in individual patients, and to facilitate the selection of patient-specific therapies.

Keywords

Multiple Sclerosis, Retinal Nerve Fiber Layer, Optical Coherence Tomography, Optic Nerve, Longitudinal Study, Genetic Algorithm

INTRODUCTION

Multiple sclerosis (MS) is a degenerative disease that affects the central nervous system (CNS) and is characterized by nerve fiber inflammation and demyelination and by axonal degeneration. As a result of these phenomena, neurons partially or completely lose their ability to conduct nerve impulses, giving rise to the various symptoms of this pathology [1].

Several studies [2–4] have demonstrated increased thinning of the retinal nerve fiber layer (RNFL) in MS patients versus healthy controls. The mechanism by which this thinning occurs in MS patients that have not experienced an episode of optic neuritis remains unclear. Because the RNFL is composed of the unmyelinated axons of the retinal ganglion cells (RGCs) that form the optic nerve, thinning of this layer may be linked to the aforementioned phenomena of inflammation and axonal degeneration [5].

Several longitudinal studies have shown that the decrease in RNFL thickness in MS patients exceeds that associated with ageing [6–8]. A follow-up study of 61 patients [7] found that the progressive decrease in RNFL thickness was more pronounced in MS patients than in aging healthy controls. Similarly, Talman et al. [8] described a decrease in RNFL thickness of 2 µm/year in MS patients, as compared with 0.49 µm over 3 years in controls.

There are numerous non-invasive imaging techniques currently available that allow measurement of the thickness of the different retinal layers. The most widespread technique is optical coherence tomography (OCT) [9], which is used to diagnose and monitor multiple diseases of the retina and optic nerve [5].

A key use of OCT in monitoring MS progression is to determine whether variations in RNFL thickness are linked to irreversible damage caused by the disease or, conversely, are the result of acute episodes of the disease. It has been shown that a single episode of optic neuritis does not imply a greater risk of a progressive decrease in RNFL thickness [10].

In this study, we focus on the mechanisms that cause thinning of the unmyelinated fibers that comprise the RNFL. Because the interaction and evolution of the inflammatory and degenerative processes caused by MS are poorly understood, is particularly difficult to predict the course of MS [11]. Several hypotheses have been proposed to explain the dynamics of MS: some consider the underlying pathological changes to be the result of simultaneous inflammatory and degenerative processes, while others propose that the disease course consists of a series of discrete phases [12,13]. Regardless, it is clear that CNS damage in MS is caused by acute inflammatory processes initiated by the immune system and by axonal degeneration caused by demyelination [14,15].

Recently, Kotelnikova et al. [16] hypothesized that the evolution of MS is driven by an autoimmune response against the CNS itself that causes inflammation, axonal degeneration, and loss or regeneration of myelin. They concluded that the manner in which each process occurs varies between different clinical

subgroups. They designed a mathematical model to explain experimental data derived from brain magnetic resonance images (MRI) [17] obtained from a longitudinal study of 66 MS patients. Other studies have attempted to establish whether there is any relationship between RNFL thickness and patient disability, as measured using the Expanded Disability Status Scale (EDSS) in transversal studies, but failed to produce sufficiently robust data [18,19].

In the present study, we propose a mathematical model that relates axonal degeneration to disease progression in MS patients. This model is consistent with clinical data obtained in a longitudinal study of 114 MS patients over 10 years, and distinguishes between the relative contributions of different biological processes (inflammation, axonal degeneration, and axonal regeneration) in different patient groups. Two novel aspects of this study underscore its importance in furthering our understanding of MS. First, we have exploited the accessibility of the retina, which provides a window into the brain, in order to develop the first mathematical model to analyze CNS damage (RNFL thinning) in MS patients, [20,21]. Second, we have used OCT data to distinguish between the different biological processes that contribute to RNFL thinning.

The ultimate goal of this research is to obtain a validated numerical model that can predict the evolution of RNFL thinning in new MS patients using only OCT data and EDSS scores obtained at their first visit. RNFL thinning is known to be linked to the progression of MS-associated disease disability [18]. Sufficient control of disease activity in MS patients is crucial to prevent unfavorable outcomes. Therefore, our model could be highly useful to clinicians, helping

them to establish patient-specific treatments and deciding between first- and second-line therapies.

MATERIALS AND METHODS

Longitudinal study

The longitudinal study followed a cohort ("discovery cohort") of 114 MS patients from the Miguel Servet University Hospital (Zaragoza, Spain). All patients underwent complete ophthalmologic evaluations during the course of the 10 year follow-up period (baseline, 2.5 years, 5 years, and 10 years). This examination includes assessment of best-corrected visual acuity (BCVA) using the Snellen scale, colour vision, a visual field examination, and an OCT examination. Simultaneously, the same protocol was applied to a cohort of 60 healthy control patients in order to distinguish between age-associated RNFL thinning and that caused by disease progression. Finally, 5-year follow-up data obtained from a third cohort of 70 MS patients (validation cohort) were used to validate the proposed mathematical model. From these 3 cohorts of patients of white European origin, one eye from each subject was randomly selected for analysis (excluding eyes for which previous episodes of optic neuritis were recorded) [22]; in total 244 eyes were included in the longitudinal study. The main clinical features of these 3 cohorts are summarized in Table 1.

Baseline evaluation	Healthy controls (n = 60)	Discovery cohort (n = 114)	Validation cohort (n = 70)
General parameters			
Age [years]	43.0 ± 13.3	41.3 ± 10.5	43.1 ± 10.3
Sex (M - F)	10 - 50	32 - 82	28 - 42
BCVA [Snellen]	0.972 ± 0.219	0.846 ± 0.205	0.837 ± 0.335

MS parameters			
Disease duration [years]	–	10.5 ± 7.9	9.2 ± 9.2
Subtypes (RR - SP - PP)	–	104 - 8 - 2	65 - 4 - 1
EDSS	–	2.5 ± 2.1	2.7 ± 2.1
OCT parameters – RNFL thickness			
Mean thickness [µm]	100.93 ± 10.30	89.99 ± 18.84	89.72 ± 12.82
Superior thickness [µm]	123.36 ± 18.34	110.11 ± 23.91	114.16 ± 19.82
Nasal thickness [µm]	79.53 ± 15.62	74.75 ± 21.50	72.55 ± 13.90
Inferior thickness [µm]	131.55 ± 17.58	115.96 ± 27.99	114.34 ± 18.63
Temporal thickness [µm]	71.13 ± 19.09	60.08 ± 20.17	57.16 ± 16.76

Table 1. Clinical parameters, multiple sclerosis (MS) data, and retinal nerve fiber layer (RNFL) measurements determined using optical coherence tomography (OCT) for the baseline visit of healthy controls and the discovery and validation cohorts. Data for MS patients (discovery and validation cohorts) also include disease duration, MS subtypes (RR, relapsing-remitting; SP, secondary-progressive; PP, primary-progressive) and EDSS scores.

The required inclusion criteria were as follows: BCVA of 20/40 or higher; refractive error within ±5.00 diopters equivalent sphere and ±2.00 diopters astigmatism; and transparent ocular media (nuclear color/opalescence, cortical or posterior subcapsular lens opacity <1), according to the Lens Opacities Classification System III system [23]. Exclusion criteria included previous intraocular surgery, diabetes or other diseases affecting the visual field or nervous system, any optic neuritis episode in the 6 months preceding inclusion in the study, and ongoing use of medications that could affect visual function.

All subjects gave prior consent to participate in this study, which was conducted in accordance with the Declaration of Helsinki, and the protocol was approved by the Ethics Committee for Clinical Research of Aragon (CEICA) for the protection of human subjects. After the baseline visit, patients were evaluated 2.5, 5, and 10 years later in order to assess changes in RNFL thickness and EDSS score. The ophthalmologic evaluation was performed by an

ophthalmologist expert in MS and the EDSS score was determined by a neurologist.

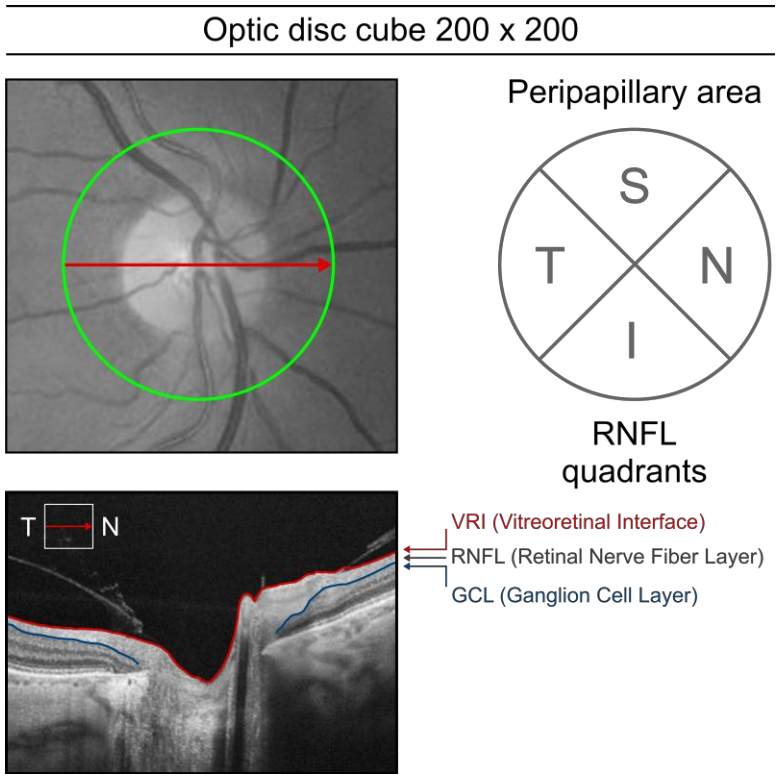

Figure 1. Optic disc cube 200 × 200 scan protocol (right eye). This peripapillary scanning protocol centers on the optic nerve and determines the thickness of the retinal nerve fiber layer (RNFL) in each of 4 quadrants (S, superior; N, nasal; I, inferior; T, temporal) into which the peripapillary area is divided, based on which the total mean RNFL thickness is calculated. The RNFL is delimited by the vitreoretinal interface (VRI, red line) and the ganglion cell layer (GCL, blue line).

The objective of this study was to characterize the relationship between RNFL thinning and MS disease progression, and thereby assess the utility of RNFL thickness as biological marker of disease progression. RNFL thickness was measured using Cirrus HD-OCT technology (model 4000; Carl Zeiss Meditec, Dublin, CA). Specifically, we used the Optic Disc Cube 200 × 200 study protocol, which scans an area of 6 × 6 mm centered on the papilla, capturing a data cube of 200 × 200 sweeps for a total of 40,000 data points in 1.5 seconds. The image quality is based on the signal strength measurement, which combines the signal-to-noise ratio with the uniformity of the signal within a scan.

The quality score ranges from 0 (poor) to 10 (excellent). Only images with a quality score of ≥7 were included in our analysis. The OCT system automatically identifies the center of the papilla and creates a circle-shaped sweep of 3.46 mm in diameter. This protocol calculates mean RNFL thickness by first determining the values corresponding to each of 4 quadrants into which the peripapillary area is divided (Figure 1).

Clustering of patients

To reduce the high level of clinical heterogeneity among patients, clustering of the patients in the discovery cohort was performed using the k-means clustering algorithm, which assigns patients to k sub-groups based on proximity to the mean value of a given sub-group. The k-means clustering algorithm is one of the most commonly used techniques for this purpose, owing to its ability to quickly and efficiently segment large samples, including outliers. Since this method is highly sensitive to the initial number of groups assigned, the algorithm was executed several times using k-values (i.e. number of clusters) ranging from 2–10. The Silhouette method was used to validate the number of groups that best classified the data set. This method measures how close each data point is to its own cluster and its closest neighbors in order to determine the optimum k-value. Silhouette analysis is widely used in the evaluation of k-means clustering since it is faster and more cost-effective than other available methods (e.g. cost function analysis) [24].

The proposed methodology was developed to predict the evolution of RNFL thickness in new MS patients after their first visit. Baseline parameters were used to classify patients. We applied a 3D classification procedure using the

following variables: EDSS score (patient´s disability is related to axonal damage [2]); BCVA (50% of patients present some form of visual impairment); and disease duration ratio (time since disease onset relative to patient's age), which represents the proportion of patient's life spent with MS.

Mathematical model

In this section we describe the development of a mathematical model to characterize the evolution of RNFL thickness in MS patients.

Biological considerations

At disease onset, the predominant pathological consequences of MS are demyelination and axonal transection (i.e. complete and transversal section of the nerve fiber). However, as the pathology progresses, CNS inflammation and axonal degeneration predominate [25]. Unlike the study performed by Kotelnikova et al. [16], which modeled inflammatory attack, demyelination, remyelination, and nerve fiber loss, our model does not account for myelin-related processes, since RNFL nerve fibers are unmyelinated.

The proposed mathematical model, based on ordinary differential equations (ODEs), comprises 3 processes thought to be implicated in the evolution of the RNFL thinning in MS patients: autoimmune inflammation; axonal degeneration; and axonal regeneration. While autoimmune inflammation occurs in all forms of MS, its overall contribution relative to axonal degeneration and regeneration, as well as its temporal profile, can vary from one patient to the next [26]. By contrast, axonal degeneration does not follow autoimmune dynamics: damage accumulates as a consequence of the poor regenerative capacity of the CNS

[15]. As is well documented, both inflammation and axonal degeneration cause numerous types of disabilities [26]. Finally, while axonal regeneration and functional recovery can occur in the peripheral nervous system (PNS), the regenerative capacity of the CNS after injury is very limited [27].

We distinguish between healthy axons, which have not yet been affected by the disease, and damaged axons, which decrease in thickness as a consequence of the inflammatory process (see Figure 2). A and A_d represent the proportion of the total RNFL thickness corresponding to healthy and damaged axons, respectively. The temporal evolution of these parameters is described by the following equations:

$$\frac{dA}{dt} = -k_{inf} AR(t) A + k_{reg} A_d - k_{degA} A \quad (1)$$

$$\frac{dA_d}{dt} = k_{inf} AR(t) A - k_{reg} A_d - k_{degA_d} A_d \quad (2)$$

where the constant k_{inf} and the time-dependent parameter autoimmune response $AR(t)$ represent the inflammation process. Thus, healthy axons that are affected by an inflammatory outbreak or by progressive inflammation become damaged axons, with subsequent loss of volume and even total transection of the nerve fiber. The constants k_{degA} (healthy axons) and k_{degAd} (damaged axons) model axonal loss by volume reduction or axonal transection. Finally, the poor regeneration of damaged axons, which can partially recover from an inflammatory episode, is represented by constant k_{reg}.

Axonal degeneration D is defined as the process by which axons decrease in size, ultimately atrophying and degenerating:

$$\frac{dD}{dt} = k_{degA}A + k_{degA_d}A_d \quad (3)$$

Note that both axonal degeneration and transection cause problems in the CNS by impairing the transmission of nerve impulses.

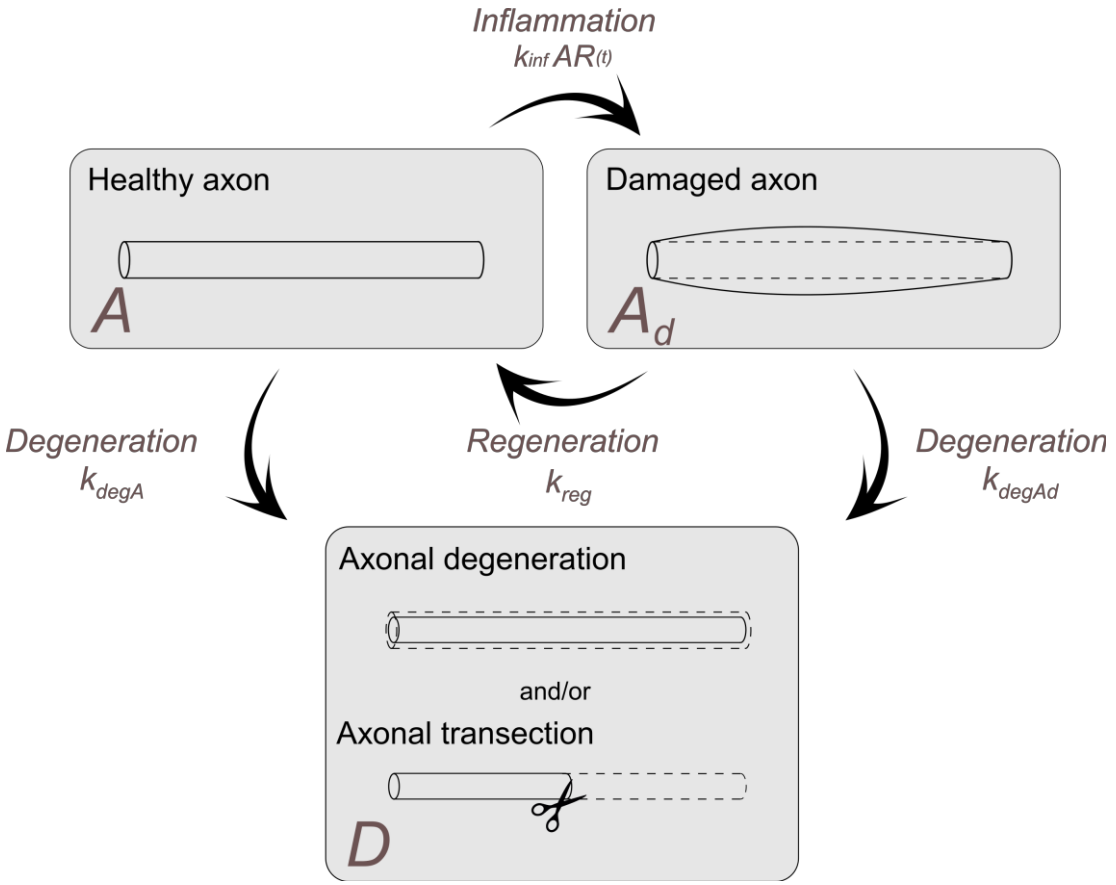

Figure 2. Graphical representation of the proposed mathematical model. The model represents the evolution in MS patients of the thickness of the RNFL, which is composed of healthy axons (A) and by axons affected by autoimmune inflammation (A_d). The inflammatory process is modeled by the autoimmune response $AR(t)$ and constant k_{inf}. Both healthy and damaged axons can decrease in volume as a result of axonal degeneration or transection (D), according to constants k_{degA} and k_{degAd}, respectively. A small proportion of damaged axons can regenerate, recovering their initial volume: constant k_{reg} represents this weak regenerative capacity.

Representation of autoimmune inflammation

Autoimmune inflammation is represented by EDSS scores obtained during the 10-year follow-up of the discovery cohort, since progression of this score correlates with a significant change in neurological status [28]. Hence,

incremental changes in disability (ΔEDSS) were considered when EDSS score increased by ≥1 between visits (selection of larger increments would exclude patients with slower progressing disability). Autoimmune inflammation is modeled considering the time between changes in EDSS score. Time intervals (ΔT) between ΔEDSS were computed. Mean ΔT values were calculated for each patient in the discovery cohort. These data were grouped by clustering and then the probability distribution that best fit these experimental values was determined. By adjusting *AR(t)* to these probability distributions, we can represent the autoimmune inflammation that corresponds to an increase in disability and consequently, in EDSS score. Thus, in our proposed model patients with more slowly progressing disability experience autoimmune inflammation later than patients with faster progressing disability.

Adaptation of the model to clinical outcomes

In order to adjust the constants of the model to the clinical data it is necessary to set boundary conditions, taking into account both biological considerations and conservation laws.

The variable measured by OCT corresponds to RNFL thickness. In our numerical model, this thickness is the sum of the thickness of both healthy and damaged axons:

$$A_t(t) = A(t) + A_d(t) \quad (4)$$

In all simulations, we assume that all axons are healthy at the start of the follow-up period and therefore that damaged axons and degeneration are absent at

baseline. The thickness measurement at baseline is thus considered the reference and the starting point:

$$A_t(0) = A(0) = baseline\ visit\ ;\ A_d(0) = D(0) = 0 \quad (5)$$

Conservation law states that the sum of healthy axons, damaged axons and degenerated axonal thickness must remain constant in time:

$$A(t) + A_d(t) + D(t) = A_t(t) + D(t) = constant \quad (6)$$

Based on data from literature, a range of values and a hierarchy between constants was defined in order to satisfy the different biological processes. Because the rate of CNS regeneration is very low [27], this parameter will have the smallest value (range, 0–0.0001). For axonal loss, the parameters represent the percentage of healthy or damaged axons involved in each process, and therefore the corresponding values can range from 0 (no axonal loss) to 1 (entire volume of the axon is affected) [1]. Finally, autoimmune inflammation is represented by the constant k_{inf} (range, 0–10) and the autoimmune response *AR(t)* [16]. The units of all constants are 1/day since thickness is measured in µm and its evolution is expressed in µm/day.

Optimization of model parameters

An optimization algorithm was used to determine the optimal parameters for the proposed model, minimizing the root mean square error (RMSE) between the values predicted by our mathematical model and the clinical data. RMSE quantifies the difference between analytical and experimental values in units of thickness. Specifically, Matlab (version R2017b, Mathworks Inc., Natick, MA) was used to implement a genetic algorithm based on natural selection and

genetics, and designed to drive evolution of an initial population towards optimal fitness. This use of this type of algorithm for a similar purpose has been previously described [29].

For the purposes of our analysis, the chromosome is composed of our 4 constants (k_{inf}, k_{reg}, k_{degA} and k_{degAd}). Each individual is represented by 56 bits, which corresponds to the binary coding of these 4 constants. The selection method used was fit-fit, whereby the most competitive individuals cross with the best and the least competitive with the worst. For the creation of new individuals, the 2-point crossover operator was used for binary coding, where children contain entire variables of both parents [30]. To avoid the loss of diversity that crossing processes can cause and to prevent blocking of the algorithm, a mutation probability of 20% was established. Mutation was applied to new descendants, introducing a random modification in one or several genes.

An optimization cycle was simulated for each group of patients and for each zone of the peripapillary area, with 100 iterations and a population size of 1000 individuals, since in this problem the initial population had a greater influence on the results than the number of iterations.

RESULTS

Longitudinal study

Differences in the evolution of RNFL thickness between the discovery cohort and healthy controls were compared using the Wilcoxon test (p-values <0.05 were considered significant). The mean and standard deviation were computed for each cohort and for different peripapillary areas. As described in the

Supplementary Material (Figure 1S), thinning of the RNFL in both MS patients and controls was observed between the baseline and 10-year follow-up visits, confirming that natural aging is an important component of this phenomenon. However, as also described previously [31], this thinning was of a greater magnitude in MS patients, confirming that RNFL thinning is also caused by MS progression. Specifically, at baseline mean RNFL thickness was 10.89% lower in MS patients than in respect to healthy controls. The reduction in RNFL thickness was even more pronounced at the 10-year follow up visit (7.80% and 14.12% decreases relative to corresponding baseline values in controls and MS patients, respectively).

Comparison of 10-year follow-up data for the control and MS groups revealed the following p-values: mean RNFL, 0.00029; superior RNFL, 0.0069, nasal RNFL, 0.5653; inferior RNFL, 0.0047; temporal quadrant RNFL, 0.00023. Therefore, significant differences in RNFL thinning were observed between MS patients and controls in all areas, except in the nasal quadrant.

Clustering of patients

After performing group selection using Silhouette analysis in the k-means clustering algorithm, an optimal number of 3 groups was established, with a Silhouette value of 0.8349. As shown in Figure 3, group 1 corresponds to patients who began follow-up with a higher EDSS score while group 3 corresponds to those with the least advanced disability. While subjects were classified using other variables and different combinations thereof, the resulting Silhouette values were always lower than 0.8349.

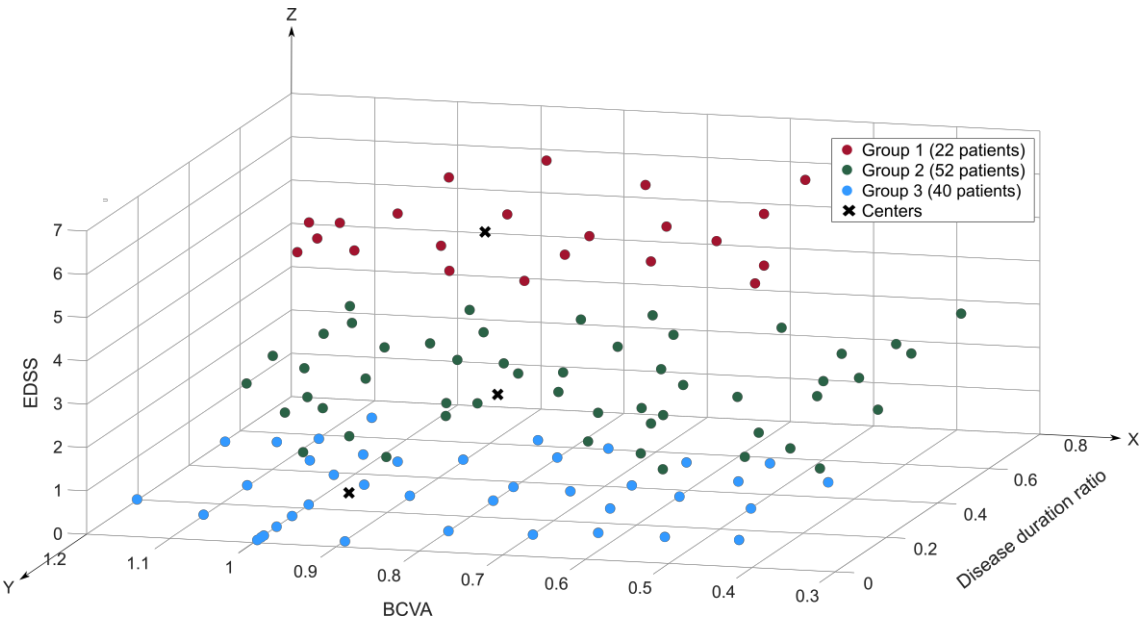

Figure 3. Clustering of patients into the optimal number of groups according to Silhouette criterion. 3D classification was performed using the following variables: BCVA (X axis), disease duration ratio (Y axis), and EDSS score (Z axis). Patient clustering was as follows: group 1, 22 patients (age, 45.7 ± 11.9; disease duration, 14.7 ± 10.6; EDSS, 6.1 ± 0.3); group 2, 52 patients (age, 41.7 ± 9.2; disease duration, 11.1 ± 7.6; EDSS, 2.6 ± 0.6); group 3, 40 patients (age, 38.3 ± 11; disease duration, 7.2 ± 5; EDSS, 0.5 ± 0.5).

Once patients in the discovery cohort were grouped into different clusters, the evolution of RNFL thickness over the 10-year follow-up period could be analyzed. Figure 2S shows the temporal evolution (baseline and 2.5, 5, and 10 years) of RNFL thickness for each group and for each quadrant of the peripapillary area. These values always decrease over time. To provide a comprehensive overview of RNFL thinning in MS patients, these data are summarized in Table 2, which shows the percentage decrease over the 10-year follow-up period. Group 1 shows a smaller decrease in RNFL thickness in 4 of the 5 areas analyzed with respect to group 2, and in all 5 areas with respect to group 3. RNFL thinning in the peripapillary area in group 1 was 1.64 times lower than that observed in group 2, which in turn was 1.14 times lower than that observed in group 3. Taken together these data reveal a lower magnitude of RNFL thinning in patients who began the follow-up period with greater disability (group 1). Therefore, most of this thinning occurs during the initial stages of

disability (groups 2 and 3). However, the differences in RNFL thinning between the 3 patient groups were not significant (p>0.05).

RNFL thinning [µm]	*Group 1*	*Group 2*	*Group 3*
Peripapillary area	7.67 (9.1%)	13.20 (14.9%)	17.07 (17.0%)
Superior quadrant	7.50 (7.1%)	14.50 (13.6%)	24.00 (19.8%)
Nasal quadrant	6.50 (9.1%)	9.50 (13.3%)	14.50 (17.3%)
Inferior quadrant	6.50 (5.7%)	11.00 (9.6%)	20.00 (16.0%)
Temporal quadrant	9.50 (17.3%)	8.00 (14.3%)	15.00 (21.4%)

Table 2. Decrease in retinal nerve fiber layer (RNFL) thickness in the entire peripapillary area and in the 4 quadrants into which it is divided. Values represent the median thinning in µm during the 10-year duration of the longitudinal study. The decrease observed over the 10-year follow-up period is represented as a percentage of baseline RNFL thickness.

Furthermore, Figure 2S shows that in all 3 groups the evolution of RNFL thickness follows a linear trend during follow-up. The negative slope of this trend decreases as the initial EDSS score increases.

Mathematical model

The autoimmune response *AR(t)* is assumed to be defined by the probability distribution that best fits the clinical data. For group 1, the distribution is an extreme value distribution, with the following probability density function:

$$AR(t)_1 = \sigma^{-1} e^{\frac{t-\mu}{\sigma}} e^{-e^{\frac{t-\mu}{\sigma}}} = 677.7^{-1} e^{\frac{t-2711.8}{677.7}} e^{-e^{\frac{t-2711.8}{677.7}}} \quad (7)$$

For groups 2 and 3, the optimal fits are Weibull and Rayleigh distributions, respectively:

$$AR(t)_2 = \frac{b}{a}\left(\frac{t}{a}\right)^{b-1} e^{-\left(\frac{t}{a}\right)^b} = \frac{3.2}{1947.2}\left(\frac{t}{1947.2}\right)^{3.2-1} e^{-\left(\frac{t}{1947.2}\right)^{3.2}} \quad (8)$$

$$AR(t)_3 = \frac{t}{\sigma^2} e^{\frac{-t^2}{2\sigma^2}} = \frac{t}{818.7^2} e^{\frac{-t^2}{2 \cdot 818.7^2}} \quad (9)$$

Figure 4 shows clinical data for each group of the discovery cohort and the optimal distribution for these data. Each bar represents the probability density of the number of days between changes in EDSS score. These distributions reflect the rate of EDSS increase. Thus, group 3 has the highest probability of a 1-point increase in EDSS score (818.7 days) while group 1 has the lowest (2711.8 days). Therefore, the progression of disability in patients in the initial stages of the disease is faster than that observed in patients with higher EDSS scores. This observation is also reflected in the slope of the linear approximation for EDSS score evolution; this slope decreases as the disability state increases.

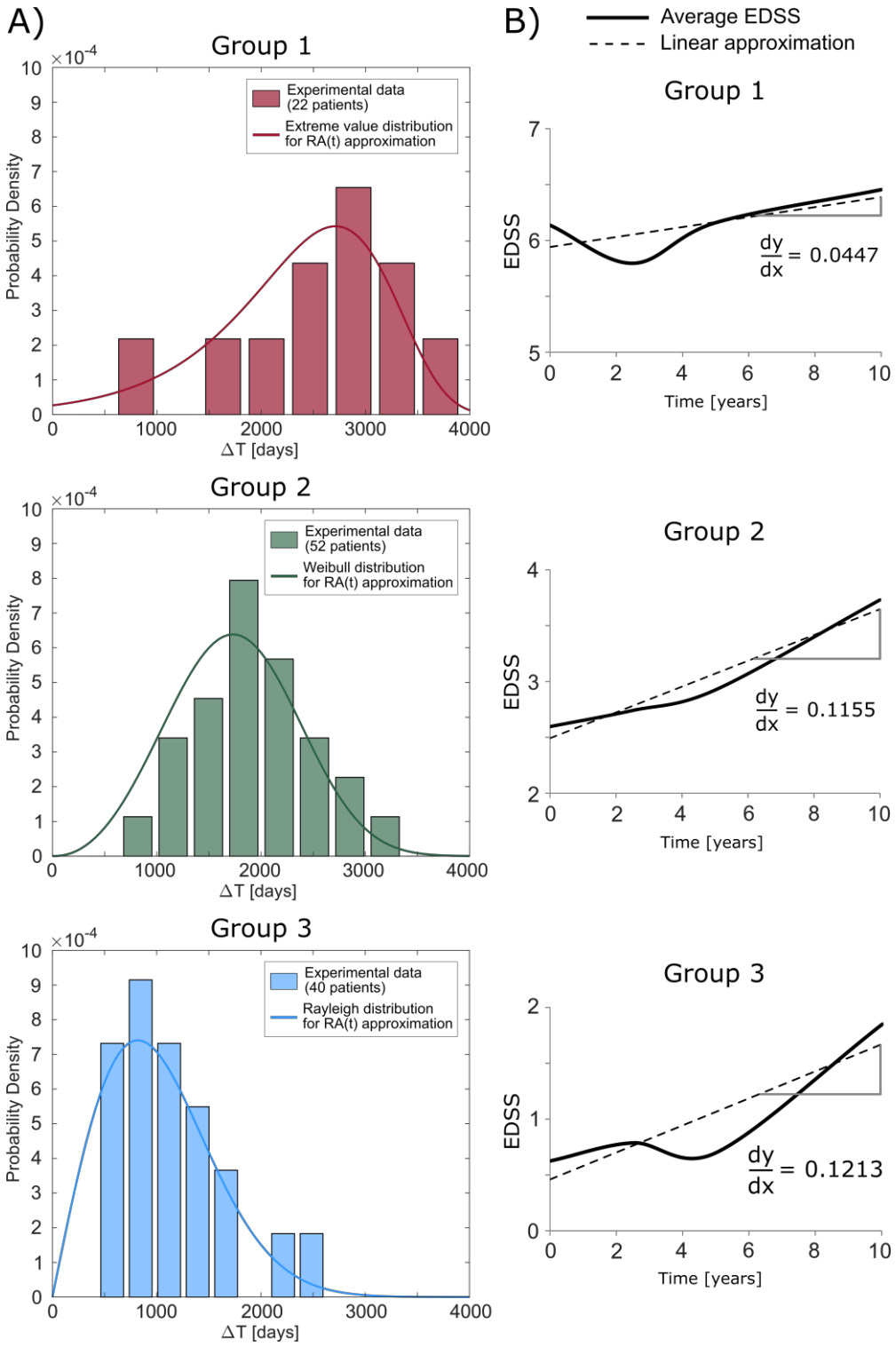

Figure 4. A) Distribution of ΔT values for increments ≥1 point on the Expanded Disability Status (EDSS) scale for each group in the discovery cohort. The following probability density functions best fit each group: group 1, extreme value distribution; group 2, Weibull distribution; group 3, Rayleigh distribution. B) Evolution of mean EDSS score for each group for the 10-year follow-up period. Dashed line represents the linear approximation of EDSS score evolution.

After defining the autoimmune response, it is necessary to determine the constants for the model by adjusting it to the clinical data from the discovery

cohort. These parameters were optimized using our genetic algorithm. The best adjustment for these 4 constants (k_{inf}, k_{reg}, k_{degA} and k_{degAd}) is shown in the Supplementary Material (Table 1S). In all cases the RMSE value obtained to fit the mathematical model to the clinical data was very low. The maximum RMSE value was 2.30 µm for the superior quadrant of group 1 and the minimum value was 0.12 µm for the peripapillary area of group 2. The values obtained for these constants are also shown in Figure 5. To identify the biological processes that most influence the dynamics of each group, we compared the parameters corresponding to each of the different processes between groups. We found that patients with greater disability experienced less autoimmune inflammation (k_{inf}(group1) < k_{inf}(group2) < k_{inf}(group3)), and that consequently the number of damaged axons slowly increased in group 1 (k_{degAd}(group1) < k_{degAd}(group2, group3)). A similar trend was observed for the degeneration of healthy axons (k_{degA}(group1) < k_{degA}(group2) < k_{degA}(group3)), revealing that axonal degeneration in MS patients is greater during early disease stages. However, the degeneration of damaged axons did not follow this same trend: in this case, the degeneration of damaged axons was greater in group 2 than group 3 (k_{degAd}(group2) > k_{degAd}(group3)).

Finally, we observed that the regeneration process was consistent with the degree of disability: patients with lower EDSS scores had a greater regenerative capacity than patients with higher EDSS scores (k_{reg}(group1) < k_{reg}(group2) < k_{reg}(group3)).

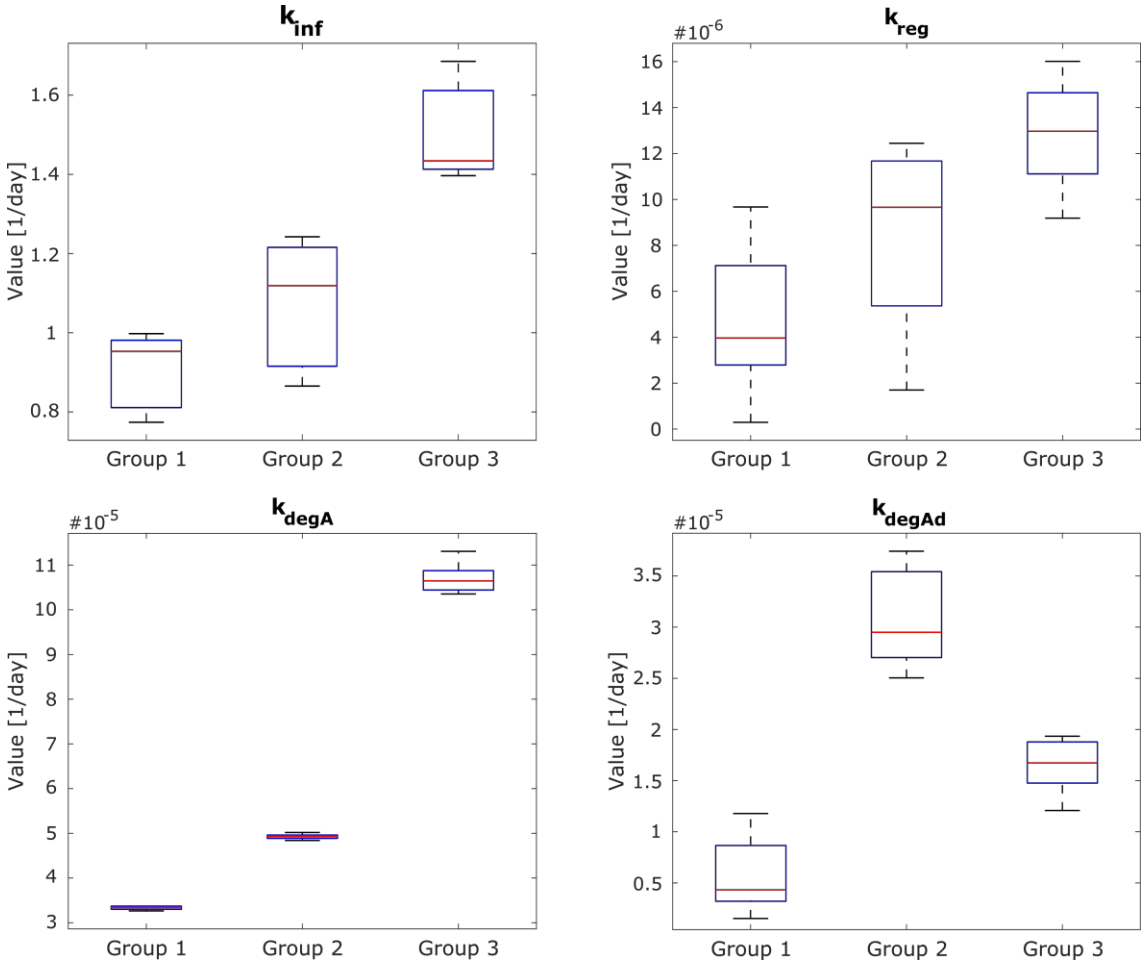

Figure 5. Parameter distribution for the 3 groups of patients in the discovery cohort. This box-diagram was generated using the 10 best combinations of parameters (values are shown in Table 1S). Autoimmune inflammation is represented by k_{inf}, constants k_{degA} and k_{degAd} relate to axonal degeneration, and k_{reg} is the regeneration ratio.

The evolution of each axon type (healthy or damaged) included in our model is depicted in Figure 6. This mathematical model allows determination of the evolution of healthy and damaged axons. Therefore, the sum of the thicknesses of each of these axon types should correspond to the experimental RNFL thickness measured by OCT. As shown in Figure 6 (right panel), the evolution of RNFL thickness as determined numerically fit precisely with the OCT clinical data. Our model can be adjusted to the RNFL thickness data for all patient groups with minimum error, verifying the model's ability to reproduce the different dynamics that occur during MS progression.

The evolution of total thickness A_t, healthy axon thickness A, damaged axon thickness A_d, and cumulative damage D are shown for each group of the discovery cohort in Figure 6 (left panel). Based on our assumption that all axons are healthy at the start of follow-up, patients with the greatest disability (group 1) experience less autoimmune inflammation caused by MS, and therefore only a small proportion of healthy axons transform into damaged axons. However, in MS patients with less disability (groups 2 and 3), the number of damaged axons increases markedly. This behavior is conditioned both by the autoimmune response $AR(t)$ and constant k_{inf}. The results obtained for groups 2 and 3 show how damaged axons, which have undergone autoimmune inflammation, are degenerated, since most of the axons affected by MS degenerate in the initial stages of the disease. After peaking, the curve representing the evolution of damaged axons in groups 2 and 3 acquires a negative slope because the rate of degeneration is greater than at the beginning. Finally, due to the aforementioned effect degeneration D is greater in patients with less disability ($D(\text{group1}) < D(\text{group2}) < D(\text{group3})$).

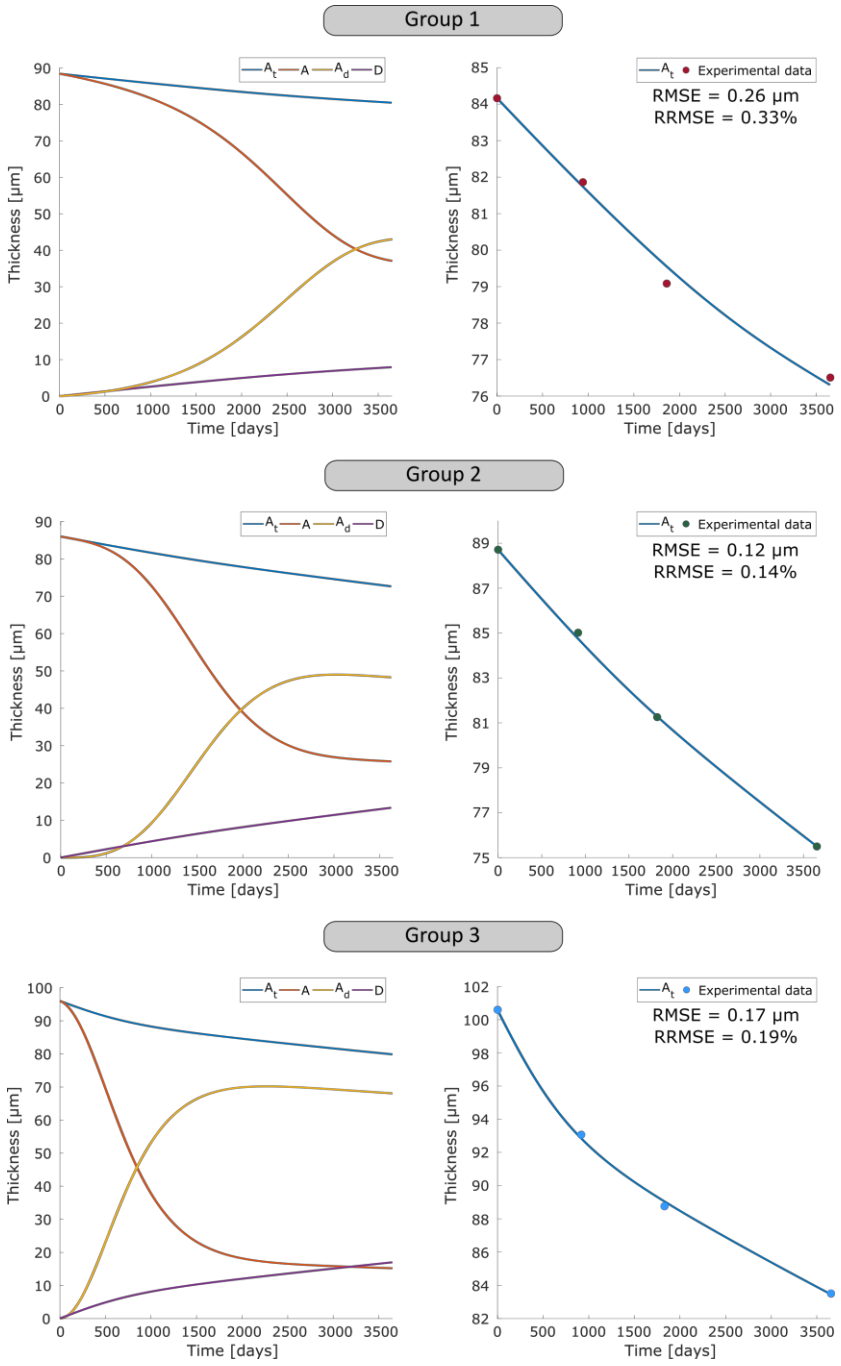

Figure 6. Theoretical-experimental comparison of the evolution of retinal nerve fiber layer (RNFL) thickness for each group. Left: temporal evolution of healthy axons *A*, damaged axons A_d, and degeneration *D*. Right: adjustment of RNFL thicknesses obtained with the numerical model to the clinical data.

Mathematical model validation

Finally, to validate the model generated using mean data from each group in the discovery cohort over the 10 years of the longitudinal study, we investigated whether the model could correctly determine the evolution of RNFL thickness in

individual patients. We calculated RMSE and relative RMSE (RRMSE) for each patient in the discovery cohort and used a bootstrap procedure to determine mean RMSE and the corresponding 95% confidence interval (CI) for each group. This bootstrap method was applied randomly, replacing the original sample 10,000 times. Using the 10-year follow-up data, the following values (shown in Figure 7) were obtained for RMSE (group 1, 2.45 µm [95% CI, 1.87–3.06]; group 2, 3.20 µm [95% CI, 2.74–3.66]; group 3, 4.01 µm [95% CI, 3.32–5.59]) and RRMSE (group 1, 3.05% [95% CI, 2.34–3.79]; group 2, 4.20% [95% CI, 3.52–4.88]; group 3, 4.48% [95% CI, 3.63–5.25]).

We also validated our proposed model using data from a new cohort of patients (validation cohort) followed-up for 5 years. First, we assigned each patient in the validation cohort to one of the 3 groups previously defined for the discovery cohort, using data recorded on their first visit. Next, for each group we computed the evolution of RNFL thickness over 5 years using our mathematical model. Finally, following the same procedure described for the discovery cohort, we compared the theoretical values obtained for the validation cohort with the corresponding clinical data. As shown in Figure 7, the mean RMSE and RRMSE values for the validation cohort were sufficiently low and very similar to those obtained for the discovery cohort. Therefore, this validation exercise revealed that our proposed model can predict RNFL thinning in new MS patients with a high level of accuracy.

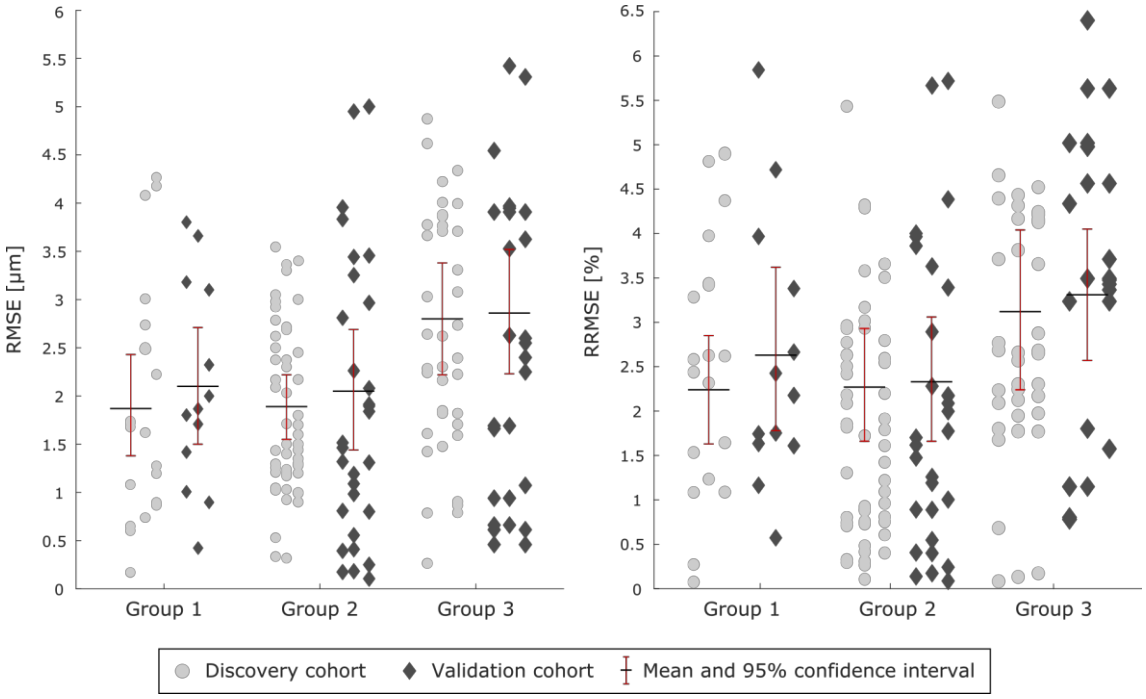

Figure 7. Root mean square error (RMSE) and relative RMSE (RRMSE) values for individual patients in the discovery and validation cohorts. Mean values and 95% confidence intervals were obtained after performing a bootstrap method with random replacement of the original sample 10,000 times.

In summary, we demonstrate that the different disease dynamics in MS patients can be represented by a combination of the 3 biological processes studied here: autoimmune inflammation, degeneration, and axonal regeneration. After clustering patients, our results indicate that RNFL thinning occurs cumulatively from the onset of MS and that most of this thinning occurs before the appearance of significant disability. In new MS patients, the proposed model allows prediction of the evolution of RNFL thickness, which in turn serves as a biomarker of MS evolution.

DISCUSSION

Using OCT to measure RNFL thickness allows direct visualization of a part of CNS. Because the RNFL is composed of unmyelinated axons, this parameter can serve as a measure of axonal loss in MS patients [32]. The use of OCT as

a biomarker of MS progression has been previously demonstrated [18]. Long-term OCT studies could provide a useful means of evaluating axonal degeneration and MS progression, and objectively assessing treatment response in MS patients.

The many commercially available OCT devices include OCT Triton, Optovue RTVue OCT, Spectralis OCT, and Cirrus HD-OCT. Our selection of Cirrus HD-OCT was based on the results of a study [33] that compared these 4 OCT devices, analyzing several parameters, and found that Cirrus HD-OCT performed best.

We used OCT data to relate RNFL thinning with disease progression in MS patients. It is well known that RNFL thinning occurs as part of normal aging. A longitudinal study of 187 eyes of healthy patients performed by Parikh et al. [34] found that mean RNFL thickness decreased by 0.16 µm/year. In our study, healthy controls showed a mean decrease of 7.86 µm over 10 years, as compared with a decrease of 12.59 µm in MS patients. These results show that pathophysiological mechanisms associated with MS cause axonal damage. Similar conclusions were reached in previous studies in which RNFL thickness in MS patients was measured by OCT [4,5]. However, to date no studies have attempted to characterize differences in the underlying pathological processes among MS patients or the corresponding implications in terms of the degree of disability.

In contrast the study of Kotelnikova and coworkers, who used MRI to analyze the evolution of brain volume in MS patients [16], we developed a mathematical model using RNFL thickness data, obtained by OCT, in order to reproduce the

dynamics of CNS damage caused by MS. Our model is based on the hypothesis that MS is a dynamically heterogeneous disease, and proposes that differences in the relative contributions of 3 key mechanisms underlying RNFL thinning (autoimmune inflammation, axonal degeneration, and axonal regeneration) could account for the different disease dynamics observed among MS patients, and hence the differences between each of the 3 subgroups into which the MS patients are divided in this longitudinal study.

Before adjusting the parameters of the model using our clinical data, we sought to reduce the heterogeneity of the data by creating subgroups within the discovery cohort based on 3 parameters: the patients' degree of disability, visual function, and the length of time that they had been living with MS. Using the k-means algorithm, 3 subgroups were created. We opted not to classify patients using the 3 classic designations (relapsing-remitting MS [RRMS], secondary progressive MS [SPMS], and primary progressive MS [15]): because 91.22% of our patients had RRMS, classification using these categories would not reduce data heterogeneity.

Our model has been optimized to fit the clinical data corresponding to each of the 3 subgroups of the discovery cohort. Different optimization algorithms using stochastic search techniques, such as genetic algorithms and particle swarm optimization [35], can be used to minimize RMSE. Although genetic algorithms have a high computational cost, we chose this approach to avoid the main disadvantage of particle swarm optimization, which tends to get stuck in local minima [36,37]. Our results show that CNS damage occurs cumulatively, beginning at disease onset, and that most RNFL thinning occurs before the

onset of significant disability (i.e. while EDSS scores are low). This conclusion is in line with the findings of a review by Petzold and coworkers [5] of several cross-sectional studies, but this is the first time it has been confirmed in a longitudinal study. Therefore, following prior corroboration of the validity of RNFL thickness as a diagnostic biomarker of MS [3], we demonstrate that this parameter can also be used to predict the evolution of MS-associated disability.

Our findings provide robust evidence demonstrating that RNFL thickness differs significantly between MS patients and healthy controls, and can be used to distinguish one group from the other, as previously suggested in several studies [6–8]. However, because RNFL thickness does not differ significantly among MS patients, it cannot be used to distinguish between them. By contrast, our classification based on EDSS score allows differentiation between 3 subgroups of MS patients categorized according to the relative contributions of the different biological processes that contribute to RNFL thinning.

Our model allowed us to quantify the degree to which each different biological process (autoimmune inflammation, axonal degeneration, and axonal regeneration) contributes to the evolution of RNFL thickness in the 3 subgroups of MS patients. As the degree of disability worsens, both autoimmune inflammation and axonal degeneration attenuate, and the regenerative capacity of the CNS decreases. Therefore, patients with the highest degree of disability have the lowest regeneration ratio. Our study is the first to analyze the influence of these biological processes on RNFL thinning in MS patients.

Some limitations of our study should be noted. Given the paucity of quantitative biological data on the biological processes described, we adjusted the

parameters of the model to fit the clinical data, and then subsequently verified that the parameters were within the established range. The autoimmune response was supposed to follow the probability distribution of time intervals between incremental changes in the disability score. Thus, the inflammatory response was defined in terms of timing in order to capture the dynamics of the damage. Therefore, this assumption allows to relate the attack response to the increase of disability. Our results should therefore be considered as trends that help us better understand the evolution of RNFL thinning and the disease course of MS. Another limitation is that we cannot experimentally measure the separate proportions of healthy and damaged axons that comprise the RNFL; OCT only allows measurement of the thickness of the entire RNFL. It should also be noted that we did not model all biological processes that can cause CNS damage, instead focusing on those known to contribute to axonal damage of retinal nerve fibers in MS. Although EDSS scores and disease duration varied considerably between patients at the beginning of follow-up, our clustering method classified patients according to disease status at baseline (including EDSS score and disease duration ratio). Therefore, differences in disease status between patients should not affect our results, and, consequently, RNFL evolution was calculated using parameters specific to each sub-group. Moreover, the same initial boundary conditions were applied to all groups, since no data on the percentage of damaged axons at the beginning of follow-up were available. Further research will be required to identify the specific regions of the RNFL in which damage occurs. Finally, parameters such as age, disease duration, and degree of disability of the validation cohort were

similar to those of the discovery cohort, which may have influenced our validation process.

Future studies analyzing larger amounts of quantitative data on the biological processes underlying CNS damage in MS will facilitate the development of more specific predictive models that could be of benefit to clinicians. The use of OCT techniques in combination with our mathematical model allows prediction of the evolution of RNFL thinning. OCT is an objective, reproducible, cost-effective and noninvasive technique that can be conducted by any clinician in a few minutes, without causing the patient any discomfort. Therefore, clinicians can rapidly predict the evolution of RNFL thinning and, consequently, the course of MS-related disability. The next step will be to incorporate this mathematical model into OCT equipment in order to directly obtain a prediction of the course of RNFL thinning. This would be of significant benefit to patients, hastening the process and obviating the need for a separate data analysis process after OCT examination. Our model will also need to be validated in other populations in order to demonstrate its utility and to confirm the validity of RNFL thickness as a reliable biomarker of MS disease course that could be used to facilitate the selection of therapies specific to a given patient.

CONCLUSION

In summary, our proposed model, generated using 10-year follow-up data collected from MS patients, demonstrates that differences in the contributions of the specific biological processes analyzed here can give rise to varying dynamics of MS progression. This may help explain the high degree of clinical heterogeneity observed among MS patients. Furthermore, our results indicate

1 that the contribution of each of these biological processes varies at different
2 disease stages. MS should be considered as a progressive disease, the course
3 of which follows the dynamics of CNS damage, and therapeutic strategies
4 should seek to reduce this damage beginning in early disease stages. Our
5 results confirm that RNFL thinning occurs cumulatively from the moment of
6 disease onset. Our proposed mathematical model allows prediction in new MS
7 patients of the progression of RNFL thinning, which in turn may serve as a
8 biomarker of MS disease progression.

9

ACKNOWLEDGEMENTS

This work was supported by the Spanish Ministry of Economy and Competitiveness through project DPI 2016-79302-R, by the Spanish Ministry of Science, Innovation and Universities (grant BES-2017-080384) and by PI17/01726 (Instituto de Salud Carlos III).

REFERENCES

[1] J.D. Haines, M. Inglese, P. Casaccia, Axonal Damage in Multiple Sclerosis, Mt. Sinai J. Med. A J. Transl. Pers. Med. 78 (2011) 231–243. doi:10.1002/msj.20246.

[2] T.A.M. Siepman, M.W. Bettink-Remeijer, R.Q. Hintzen, Retinal nerve fiber layer thickness in subgroups of multiple sclerosis, measured by optical coherence tomography and scanning laser polarimetry, J. Neurol. 257 (2010) 1654–1660. doi:10.1007/s00415-010-5589-1.

[3] A. Pérez del Palomar, J. Cegoñino, A. Montolío, E. Orduna, E. Vilades, B. Sebastián, L.E. Pablo, E. Garcia-Martin, Swept source optical coherence tomography to early detect multiple sclerosis disease. The use of machine learning techniques, PLoS One. 14 (2019) e0216410. doi:10.1371/journal.pone.0216410.

[4] E. Garcia-Martin, V. Polo, J.M. Larrosa, M.L. Marques, R. Herrero, J. Martin, J.R. Ara, J. Fernandez, L.E. Pablo, Retinal Layer Segmentation in Patients with Multiple Sclerosis Using Spectral Domain Optical Coherence Tomography, Ophthalmology. 121 (2014) 573–579. doi:10.1016/j.ophtha.2013.09.035.

[5] A. Petzold, L.J. Balcer, P.A. Calabresi, F. Costello, T.C. Frohman, E.M. Frohman, E.H. Martinez-Lapiscina, A.J. Green, R. Kardon, O. Outteryck, F. Paul, S. Schippling, P. Vermersch, P. Villoslada, L.J. Balk, ERN-EYE IMSVISUAL, Retinal layer segmentation in multiple sclerosis: a systematic review and meta-analysis., Lancet. Neurol. 16 (2017) 797–

812. doi:10.1016/S1474-4422(17)30278-8.

[6] F. Costello, W. Hodge, Y.I. Pan, L. Metz, R.H. Kardon, Retinal nerve fiber layer and future risk of multiple sclerosis., Can. J. Neurol. Sci. 35 (2008) 482–487. doi:10.1017/S031716710000915X.

[7] J. Sepulcre, M. Murie-Fernandez, A. Salinas-Alaman, A. García-Layana, B. Bejarano, P. Villoslada, Diagnostic accuracy of retinal abnormalities in predicting disease activity in MS, Neurology. 68 (2007) 1488–1494. doi:10.1212/01.wnl.0000260612.51849.ed.

[8] L.S. Talman, E.R. Bisker, D.J. Sackel, D.A. Long, K.M. Galetta, J.N. Ratchford, D.J. Lile, S.K. Farrell, M.J. Loguidice, G. Remington, A. Conger, T.C. Frohman, D.A. Jacobs, C.E. Markowitz, G.R. Cutter, G.S. Ying, Y. Dai, M.G. Maguire, S.L. Galetta, E.M. Frohman, P.A. Calabresi, L.J. Balcer, Longitudinal study of vision and retinal nerve fiber layer thickness in multiple sclerosis, Ann. Neurol. 67 (2010) 749–760. doi:10.1002/ana.22005.

[9] S. Niu, Q. Chen, L. de Sisternes, D.L. Rubin, W. Zhang, Q. Liu, Automated retinal layers segmentation in SD-OCT images using dual-gradient and spatial correlation smoothness constraint, Comput. Biol. Med. 54 (2015) 116–128. doi:10.1016/j.compbiomed.2014.08.028.

[10] E. Garcia-Martin, V. Pueyo, J.R. Ara, C. Almarcegui, J. Martin, L. Pablo, I. Dolz, E. Sancho, F.J. Fernandez, Effect of optic neuritis on progressive axonal damage in multiple sclerosis patients, Mult. Scler. J. 17 (2011) 830–837. doi:10.1177/1352458510397414.

[11] A.J. Thompson, B.L. Banwell, F. Barkhof, W.M. Carroll, T. Coetzee, G. Comi, J. Correale, F. Fazekas, M. Filippi, M.S. Freedman, K. Fujihara, S.L. Galetta, H.P. Hartung, L. Kappos, F.D. Lublin, R.A. Marrie, A.E. Miller, D.H. Miller, X. Montalban, E.M. Mowry, P.S. Sorensen, M. Tintoré, A.L. Traboulsee, M. Trojano, B.M.J. Uitdehaag, S. Vukusic, E. Waubant, B.G. Weinshenker, S.C. Reingold, J.A. Cohen, Diagnosis of multiple sclerosis: 2017 revisions of the McDonald criteria, Lancet Neurol. 17 (2018) 162–173. doi:10.1016/S1474-4422(17)30470-2.

[12] C. Louapre, C. Lubetzki, Neurodegeneration in multiple sclerosis is a process separate from inflammation: Yes, Mult. Scler. J. 21 (2015) 1626–1628. doi:10.1177/1352458515587598.

[13] E. Leray, J. Yaouanq, E. Le Page, M. Coustans, D. Laplaud, J. Oger, G. Edan, Evidence for a two-stage disability progression in multiple sclerosis, Brain. 133 (2010) 1900–1913. doi:10.1093/brain/awq076.

[14] A. Bar-Or, J.P. Antel, Central nervous system inflammation across the age span, Curr. Opin. Neurol. 29 (2016) 381–387. doi:10.1097/WCO.0000000000000331.

[15] G. Giovannoni, G. Cutter, M. Pia-Sormani, S. Belachew, R. Hyde, H. Koendgen, V. Knappertz, D. Tomic, D. Leppert, R. Herndon, C.A.M. Wheeler-Kingshott, O. Ciccarelli, D. Selwood, E.V. di Cantogno, A.F. Ben-Amor, P. Matthews, D. Carassiti, D. Baker, K. Schmierer, Is multiple sclerosis a length-dependent central axonopathy? The case for therapeutic lag and the asynchronous progressive MS hypotheses, Mult. Scler. Relat. Disord. 12 (2017) 70–78. doi:10.1016/j.msard.2017.01.007.

[16] E. Kotelnikova, N.A. Kiani, E. Abad, E.H. Martinez-Lapiscina, M. Andorra, I. Zubizarreta, I. Pulido-Valdeolivas, I. Pertsovskaya, L.G. Alexopoulos, T. Olsson, R. Martin, F. Paul, J. Tegnér, J. Garcia-Ojalvo, P. Villoslada, Dynamics and heterogeneity of brain damage in multiple sclerosis, PLOS Comput. Biol. 13 (2017) e1005757. doi:10.1371/journal.pcbi.1005757.

[17] M. Filippi, M.A. Rocca, O. Ciccarelli, N. De Stefano, N. Evangelou, L. Kappos, A. Rovira, J. Sastre-Garriga, M. Tintorè, J.L. Frederiksen, C. Gasperini, J. Palace, D.S. Reich, B. Banwell, X. Montalban, F. Barkhof, MRI criteria for the diagnosis of multiple sclerosis: MAGNIMS consensus guidelines, Lancet Neurol. 15 (2016) 292–303. doi:10.1016/S1474-4422(15)00393-2.

[18] E.H. Martinez-Lapiscina, S. Arnow, J.A. Wilson, S. Saidha, J.L. Preiningerova, T. Oberwahrenbrock, A.U. Brandt, L.E. Pablo, S. Guerrieri, I. Gonzalez, O. Outteryck, A.-K. Mueller, P. Albrecht, W. Chan, S. Lukas, L.J. Balk, C. Fraser, J.L. Frederiksen, J. Resto, T. Frohman, C. Cordano, I. Zubizarreta, M. Andorra, B. Sanchez-Dalmau, A. Saiz, R. Bermel, A. Klistorner, A. Petzold, S. Schippling, F. Costello, O. Aktas, P. Vermersch, C. Oreja-Guevara, G. Comi, L. Leocani, E. Garcia-Martin, F. Paul, E. Havrdova, E. Frohman, L.J. Balcer, A.J. Green, P.A. Calabresi, P. Villoslada, Retinal thickness measured with optical coherence tomography and risk of disability worsening in multiple sclerosis: a cohort study, Lancet Neurol. 15 (2016) 574–584. doi:10.1016/S1474-4422(16)00068-5.

[19] E. Garcia-Martin, D. Rodriguez-Mena, R. Herrero, C. Almarcegui, I. Dolz,

J. Martin, J.R. Ara, J.M. Larrosa, V. Polo, J. Fernández, L.E. Pablo, Neuro-ophthalmologic evaluation, quality of life, and functional disability in patients with MS, Neurology. 81 (2013) 76–83. doi:10.1212/WNL.0b013e318299ccd9.

[20] T.M. Jenkins, A.T. Toosy, Optic neuritis: the eye as a window to the brain, Curr. Opin. Neurol. 30 (2017) 61–66. doi:10.1097/WCO.0000000000000414.

[21] F. London, H. Zéphir, E. Drumez, J. Labreuche, N. Hadhoum, J. Lannoy, J. Hodel, P. Vermersch, J.-P. Pruvo, X. Leclerc, O. Outteryck, Optical coherence tomography: a window to the optic nerve in clinically isolated syndrome, Brain. 142 (2019) 903–915. doi:10.1093/brain/awz038.

[22] R.A. Armstrong, Statistical guidelines for the analysis of data obtained from one or both eyes, Ophthalmic Physiol. Opt. 33 (2013) 7–14. doi:10.1111/opo.12009.

[23] L.T. Chylack, J.K. Wolfe, D.M. Singer, M.C. Leske, M.A. Bullimore, I.L. Bailey, J. Friend, D. McCarthy, S.Y. Wu, The Lens Opacities Classification System III. The Longitudinal Study of Cataract Study Group., Arch. Ophthalmol. (Chicago, Ill. 1960). 111 (1993) 831–6. doi:10.1001/archopht.1993.01090060119035.

[24] F. Wang, H.-H. Franco-Penya, J.D. Kelleher, J. Pugh, R. Ross, An Analysis of the Application of Simplified Silhouette to the Evaluation of k-means Clustering Validity, in: P. Perner (Ed.), Springer International Publishing, Cham, 2017: pp. 291–305. doi:10.1007/978-3-319-62416-

7_21.

[25] A. Kutzelnigg, H. Lassmann, Pathology of multiple sclerosis and related inflammatory demyelinating diseases, in: Handb. Clin. Neurol., 1st ed., Elsevier B.V., 2014: pp. 15–58. doi:10.1016/B978-0-444-52001-2.00002-9.

[26] J.M. Frischer, S.D. Weigand, Y. Guo, N. Kale, J.E. Parisi, I. Pirko, J. Mandrekar, S. Bramow, I. Metz, W. Brück, H. Lassmann, C.F. Lucchinetti, Clinical and pathological insights into the dynamic nature of the white matter multiple sclerosis plaque, Ann. Neurol. 78 (2015) 710–721. doi:10.1002/ana.24497.

[27] M. Curcio, F. Bradke, Axon Regeneration in the Central Nervous System: Facing the Challenges from the Inside, Annu. Rev. Cell Dev. Biol. 34 (2018) 495–521. doi:10.1146/annurev-cellbio-100617-062508.

[28] F.D. Lublin, S.C. Reingold, J. a Cohen, G.R. Cutter, P.S. Sorensen, A.J. Thompson, J.S. Wolinsky, L.J. Balcer, B. Banwell, F. Barkhof, B. Bebo, P.A. Calabresi, M. Clanet, G. Comi, R.J. Fox, M.S. Freedman, A.D. Goodman, M. Inglese, L. Kappos, B.C. Kieseier, J.A. Lincoln, C. Lubetzki, A.E. Miller, X. Montalban, P.W. O'Connor, J. Petkau, C. Pozzilli, R.A. Rudick, M.P. Sormani, O. Stuve, E. Waubant, C.H. Polman, Defining the clinical course of multiple sclerosis: The 2013 revisions, Neurology. 83 (2014) 278–286. doi:10.1212/WNL.0000000000000560.

[29] C. Stamile, G. Kocevar, F. Cotton, D. Sappey-Marinier, A genetic algorithm-based model for longitudinal changes detection in white matter

fiber-bundles of patient with multiple sclerosis, Comput. Biol. Med. 84 (2017) 182–188. doi:10.1016/j.compbiomed.2017.03.028.

[30] P. Kora, P. Yadlapalli, Crossover Operators in Genetic Algorithms: A Review, Int. J. Comput. Appl. 162 (2017) 34–36. doi:10.5120/ijca2017913370.

[31] R. Alonso, D. Gonzalez-Moron, O. Garcea, Optical coherence tomography as a biomarker of neurodegeneration in multiple sclerosis: A review, Mult. Scler. Relat. Disord. 22 (2018) 77–82. doi:10.1016/j.msard.2018.03.007.

[32] J. Kucharczuk, Z. Maciejek, B.L. Sikorski, Optical coherence tomography in diagnosis and monitoring multiple sclerosis, Neurol. Neurochir. Pol. 52 (2018) 140–149. doi:10.1016/j.pjnns.2017.10.009.

[33] M.R. Munk, H. Giannakaki-Zimmermann, L. Berger, W. Huf, A. Ebneter, S. Wolf, M.S. Zinkernagel, OCT-angiography: A qualitative and quantitative comparison of 4 OCT-A devices, PLoS One. 12 (2017) e0177059. doi:10.1371/journal.pone.0177059.

[34] R.S. Parikh, S.R. Parikh, G.C. Sekhar, S. Prabakaran, J.G. Babu, R. Thomas, Normal Age-Related Decay of Retinal Nerve Fiber Layer Thickness, Ophthalmology. 114 (2007) 921–926. doi:10.1016/j.ophtha.2007.01.023.

[35] H. Shokri-Ghaleh, A. Alfi, A comparison between optimization algorithms applied to synchronization of bilateral teleoperation systems against time delay and modeling uncertainties, Appl. Soft Comput. 24 (2014) 447–456.

doi:10.1016/j.asoc.2014.07.020.

[36] R. Hassan, B. Cohanim, O. de Weck, G. Venter, A Comparison of Particle Swarm Optimization and the Genetic Algorithm, in: 46th AIAA/ASME/ASCE/AHS/ASC Struct. Struct. Dyn. Mater. Conf., American Institute of Aeronautics and Astronautics, Reston, Virigina, 2005. doi:10.2514/6.2005-1897.

[37] M. Schmitt, R. Wanka, Particle swarm optimization almost surely finds local optima, Theor. Comput. Sci. 561 (2015) 57–72. doi:10.1016/j.tcs.2014.05.017.

SUPPLEMENTARY MATERIAL

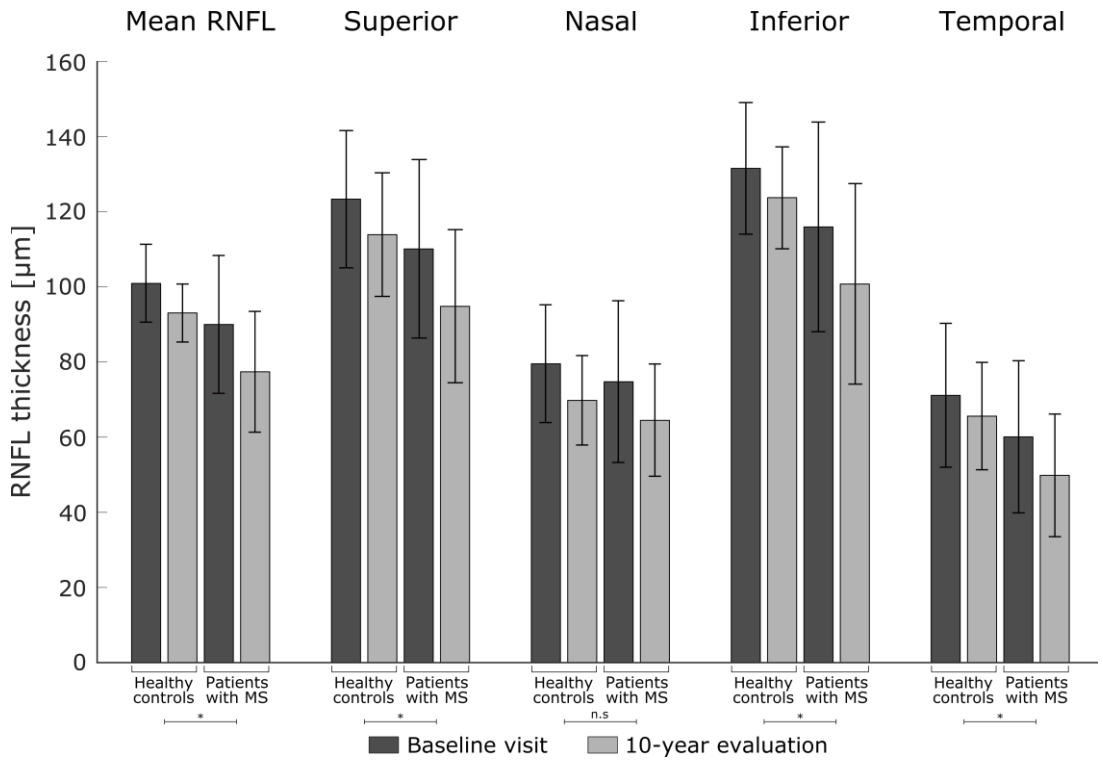

Figure 1S. Differences in RNFL thickness in MS patients and healthy controls between baseline and 10-year follow-up visits. Comparisons are shown for 4 quadrants of the peripapillary area (superior, nasal, inferior, and temporal) and for the entire peripapillary area (*p<0.05; n.s, not significant (Wilcoxon signed-rank test).

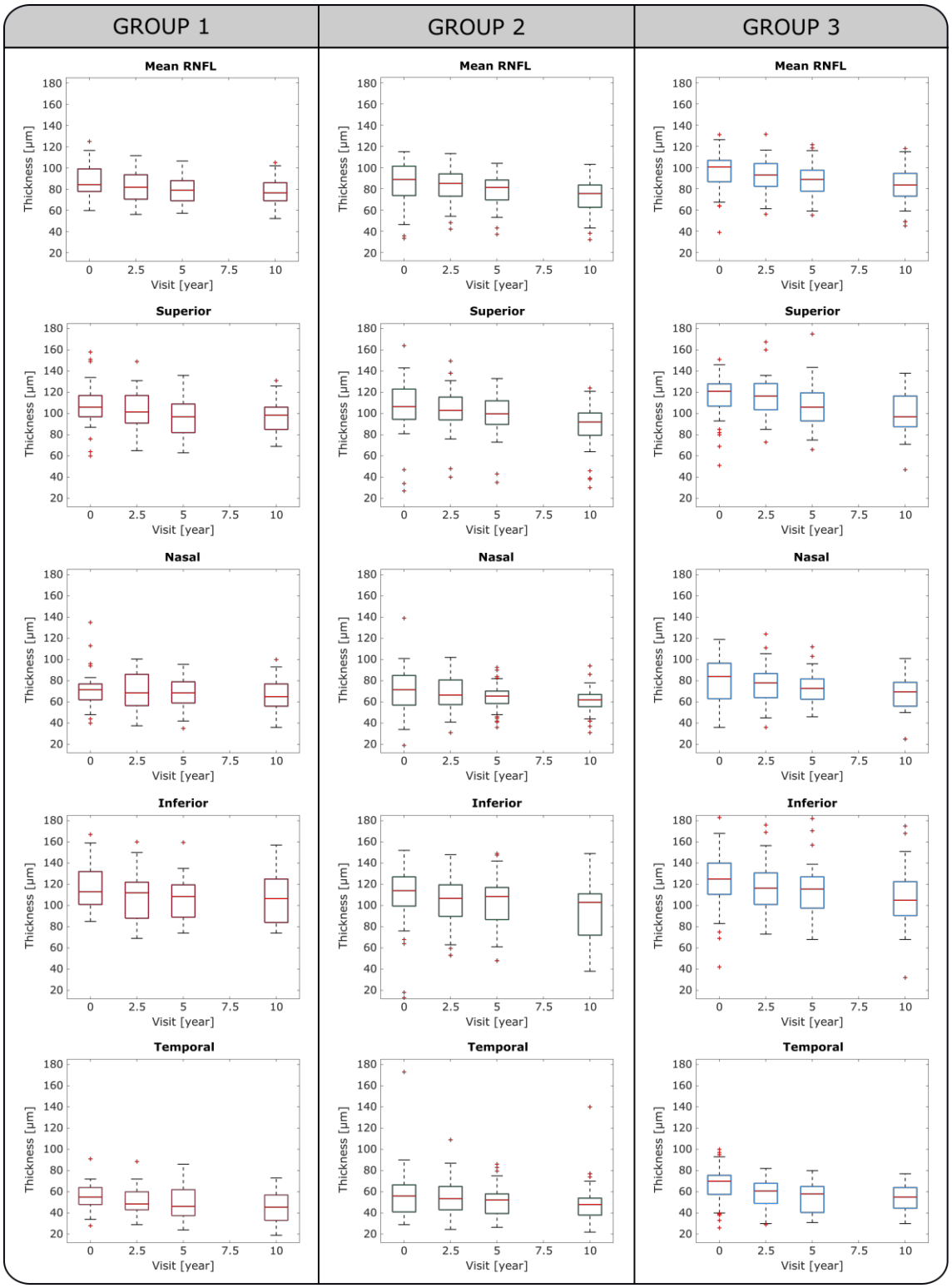

Figure 2S. Evolution of RNFL thickness in different areas for each group over 4 examinations (0, 2.5, 5, and 10 years). Red, group 1; green, group 2; blue, group 3.

Group 1				
k_{inf} [1/day]	k_{reg} [1/day]	k_{degA} [1/day]	k_{degAd} [1/day]	RMSE [µm]
Peripapillary area				
0.953	8.850E-07	3.372E-05	2.200E-06	0.26
Superior quadrant				
0.997	3.597E-06	3.308E-05	4.840E-06	2.30
Nasal quadrant				
0.918	9.695E-06	2.947E-05	1.372E-05	0.74
Inferior quadrant				
0.741	1.697E-06	1.969E-05	3.880E-06	0.69
Temporal quadrant				
1.344	2.826E-06	8.300E-05	6.860E-06	1.86
Group 2				
k_{inf} [1/day]	k_{reg} [1/day]	k_{degA} [1/day]	k_{degAd} [1/day]	RMSE [µm]
Peripapillary area				
0.914	1.080E-05	4.887E-05	3.542E-05	0.12
Superior quadrant				
0.874	2.440E-06	3.546E-05	4.946E-05	0.14
Nasal quadrant				
1.108	8.410E-07	6.154E-05	5.120E-06	0.77
Inferior quadrant				
1.207	2.310E-06	4.495E-05	2.920E-06	2.05
Temporal quadrant				
1.110	7.469E-06	4.063E-05	4.390E-05	0.32
Group 3				
k_{inf} [1/day]	k_{reg} [1/day]	k_{degA} [1/day]	k_{degAd} [1/day]	RMSE [µm]
Peripapillary area				
1.440	1.400E-05	1.068E-04	1.476E-05	0.17
Superior quadrant				
1.695	1.302E-06	5.356E-05	6.776E-05	1.73
Nasal quadrant				
1.386	2.150E-07	1.153E-04	1.296E-05	0.80
Inferior quadrant				
1.539	1.152E-05	7.381E-05	2.770E-05	1.60
Temporal quadrant				
1.386	7.649E-06	1.634E-04	8.160E-06	0.92

Table 1S. Values for the mathematical model parameters *(k_{inf}, k_{reg}, k_{deg}, k_{degAd})* that best fit RNFL thickness, as determined by OCT, for the 3 groups of patients in the discovery cohort. Fitting error is represented as the root mean square error (RMSE).